The Effect of Collagenase on the Critical Buckling Pressure of Arteries*

Ricky Martinez† and Hai-Chao Han‡

Abstract: The stability of arteries is essential to normal arterial functions and loss of stability can lead to arterial tortuosity and kinking. Collagen is a main extracellular matrix component that modulates the mechanical properties of arteries and collagen degradation at pathological conditions weakens the mechanical strength of arteries. However, the effects of collagen degradation on the mechanical stability of arteries are unclear. The objective of this study was to investigate the effects of collagen degradation on the critical buckling pressure of arteries. Arterial specimens were subjected to pressurized inflation testing and fitted with nonlinear thick-walled cylindrical model equations to determine their stress strain relationships. The arteries were then tested for the critical buckling pressure at a set of axial stretch ratios. Then, arteries were divided into three groups and treated with Type III collagenase at three different concentrations (64, 128, and 400U/ml). Mechanical properties and buckling pressures of the arteries were determined after collagenase treatment. Additionally, the theoretical buckling pressures were also determined using a buckling equation. Our results demonstrated that the buckling pressure of arteries was lower after collagenase treatment. The difference between pre- and post- treatment was statistically significant for the highest concentration of 400U/ml but not at the lower concentrations. The buckling equation was found to yield a fair estimation to the experimental critical pressure measurements. These results shed light on the role of matrix remodeling on the mechanical stability of arteries and developments of tortuous arteries.

Keywords: critical buckling pressure, mechanical stability, tortuosity, collagenase, extracellular matrix.

---

* Dedicated to Dr. Shu Chien.

† Department of Mechanical Engineering, University of Texas at San Antonio, E-mail: hchan@utsa.edu

‡ Department of Mechanical Engineering, The University of Texas at San Antonio, San Antonio, TX 78249. Tel: (210) 458-4952, Fax: (210) 458-6504, E-mail: haichao.han@utsa.edu

1 Introduction

Tortuosity is often seen in many arteries associated with arterial hypertension, aging, and atherosclerosis (1-3). Kinking of the carotid artery can lead to stroke, vertigo, syncopes, and black out (2, 4, 5). Our recent studies demonstrated that loss of stability can lead to vessel tortuosity (6-9). Therefore, it is important to further study the behavior of arterial buckling.

Collagen is a major extracellular matrix component that maintains the structure integrity and strength of blood vessels and provides the suitable environment for vascular cells. It is the major load-bearing structural element in arterial walls and collagen fiber organization is correlated with the strength of blood vessels (10). Collagen degradation, deposition, and structural alteration occur in pathological conditions and with ageing (11-13). Previous studies have shown that collagen degradation weakens the mechanical strength of the arterial wall (14, 15). However, the effects of collagen degradation on the mechanical stability of arteries remains unclear.

The objective of this study was to investigate the effects of collagen degradation on the critical buckling pressure of arteries.

2 Materials and Methods

2.1 Artery procurement and preparation

Porcine common carotid arteries were harvested from 6 to 7 month-old farm pigs (100-150 kg) post mortem at a local abattoir by midline incision. After being rinsed with PBS (Dulbecco's phosphate buffered saline, Sigma Chemical, St. Louis, MO), the specimens were placed into PBS solution and transported to our laboratory in an iced cooler. Once at the laboratory the arteries were cleaned by removing excess connective tissue and were rinsed again with PBS. Segments without side branches were selected and the *in vitro* free lengths were measured with calipers while the vessels were afloat in PBS solution. The arteries were then mounted onto a luer stopper at one end and attached to a 10ml plastic syringe filled with air at the other end and were inflated briefly to check for leaks.

2.2 Pressurized inflation testing

Arteries were subjected to pressurized inflation testing to determine their stress strain relationship (16). Briefly, arteries were inflated with PBS using a syringe and allowed to expand freely in both the circumferential and axial directions (one end was free to move longitudinally) (Fig 1). The arteries were first preconditioned by gradually inflating them with PBS to a pressure of ∼200 mmHg and deflating to

0 mmHg for 4∼6 cycles to reach a reproducible deformation. After preconditioning, initial outer diameter and axial length were measured at zero pressure. The inflation process was repeated again and recorded with a SONY digital camera at incremental steps of pressures. Later, deformed lengths and outer diameters under pressure were measured from the digital photos.
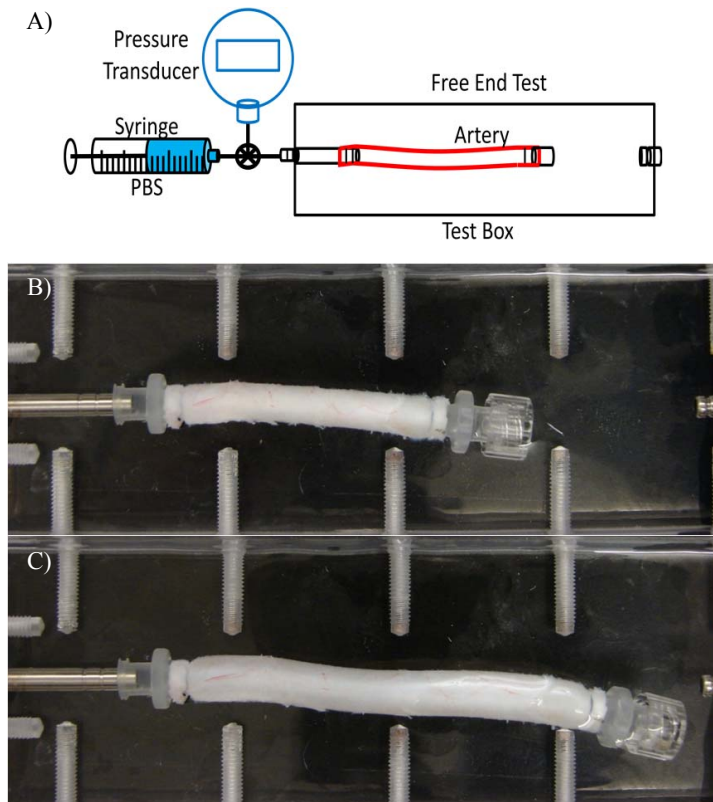

Figure 1: Top: Schematics of experimental setup for pressurized inflation test. Arteries are cannulated and pressurized with a syringe pump while one end is free to expand axially and circumferentially. Pictures: An artery during the test under a pressure of 0 mmHg (top) and 200 mmHg (bottom), respectively.

2.3 Buckling testing to determine the critical pressure

To determine the critical pressure, the arteries were tied at both ends onto cannulae inside a tissue chamber (Fig. 2). The arteries were stretched axially to designed axial stretch ratios and then gradually pressurized with PBS using the syringe pump.
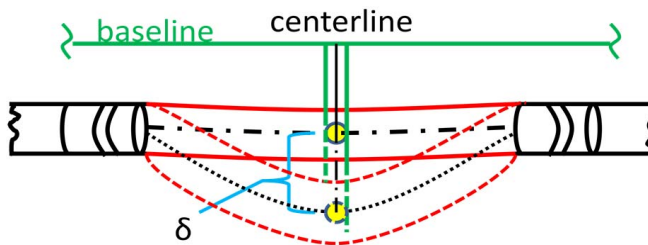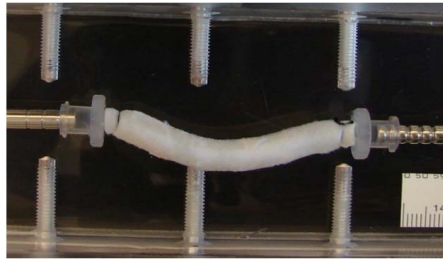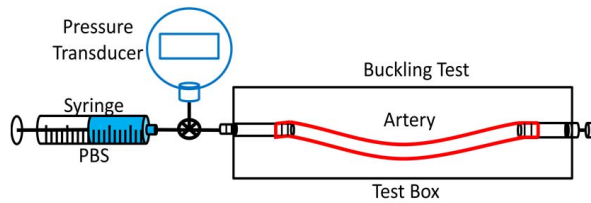
Figure 2: Top: Schematics of experimental setup for artery buckling test. Arteries are cannulated at both ends, stretched to given axial stretch ratios, and pressurized with a syringe pump. Middle: An artery buckles at a pressure of 60 mmHg (post-buckling). Bottom: Schematics illustrating the measurement of deflection (δ) of centerline of a buckled artery.

The pressure was gradually increased to generate buckling in the arteries and continued to increase beyond the critical buckling pressure to observe the post buckling behavior of the arteries. This process was repeated three times for each artery and the critical values were averaged to represent the initial reading of the critical pressure of the vessel. Then, during one loading process, photographs were taken at pressure increments using a SONY digital camera. Later, the deflections and the outer diameter of the vessel were measured from these digital photos. The critical pressure was measured as the pressure when the artery deflection (δ) becomes detectable ($\sim$0.5 mm) from an initial baseline (Fig.2) (9, 16)

2.4 Collagenase treatment

After baseline testing and measurements, arteries were treated with purified Type III Collagenase (LS005275, Worthington, Lakewood, NJ) solutions to degrade the collagen in the vessel wall (14, 17). Briefly, arteries were filled with collagenase solutions at a lumen pressure ∼55 mmHg and submerged in collagenase solutions in 10 ml test tubes to incubate at 37°C for 90-120 minutes. Three groups of arteries (n = 3, 4, 6) were treated with collagenase at concentrations of 64U/ml, 128U/ml, and 400U/ml, respectively, to achieve different levels of collagen degradation (17).

Immediately after the collagenase treatment, each vessel was washed with PBS and then tested again using inflation and buckling tests to determine the artery mechanical properties and critical buckling pressure post-treatment.

2.5 Determination of material constants and model prediction of critical pressure

The arteries are modeled as thick-walled, circular cylinders under internal pressure (p) and axial (longitudinal) tension (N) and elongated to an axial stretch ratio λ_z. The arterial wall was assumed to be incompressible, homogenous, orthotropic, nonlinear elastic and described by the Fung strain energy function w_0 (8, 18, 19)

$$w_0 = \frac{1}{2}b_0 e^Q + K[(1+2E_\theta)(1+2E_Z)(1+2E_r)-1] \tag{1}$$

$$Q = b_1 E_\theta^2 + b_2 E_Z^2 + b_3 E_r^2 + 2b_4 E_\theta E_Z + 2b_5 E_Z E_r + 2b_6 E_r E_\theta \tag{2}$$

Wherein K is the Lagrange multiplier for incompressibility, b_0, and b_1 to b_6 are material constants, and E_r, E_θ, and E_Z are the Green strains components in the radial, circumferential, and axial directions. By integrating the equilibrium equation for cylindrical artery under axial load and internal pressure, the internal pressure p and axial force N in the vessel can be expressed as (8, 18-20):

$$p = \int_{r_i}^{r_e} [(1+2E_\theta)(b_1 E_\theta + b_4 E_Z + b_6 E_r) - (1+2E_r)(b_6 E_\theta + b_5 E_Z + b_3 E_r)]B_0 e^Q \frac{dr}{r} \tag{3}$$

$$N = \pi r_i^2 p + \int_{r_i}^{r_e} [2(1+2E_z)(b_4 E_\theta + b_2 E_z + b_5 E_r)$$
$$- (1+2E_r)(b_6 E_\theta + b_5 E_z + b_3 E_r) - (1+2E_\theta)(b_1 E_\theta + b_4 E_z + b_6 E_r)]b_0 e^Q r dr \tag{4}$$

Wherein r_i, r_e are the inner and outer radii. The material constants were determined by fitting these two equations with the experimental data of pressurized inflation test using a custom programmed MATLAB code.

Then, using the material constants determined for each artery, the critical buckling pressure was determined using a buckling equation (8, 16)

$$p = \frac{N + \left(\frac{2\pi}{L}\right)^2 H}{\pi r_i^2} \tag{5}$$

Where H is the bending force due to buckling (see (8)) and N is given in Eq. 4.

2.6 *Opening angle and initial dimension measurement*

Short ring segments ($\sim$2 mm in axial length) were cut from arterial specimens to measure the opening angle of the arteries. For each vessel tested, 2-4 rings were cut from both ends of the segment before the collagenase treatment and 2-4 rings were then cut from both ends after the treatment. The rings were arranged in a petri dish filled with PBS at room temperature and each segment was cut open by a single radial cut (21). The ring sectors prop open into C-shaped configurations. After the sectors were fully relaxed for 30 minutes, the sectors were photographed to capture their zero-stress state (21). Later the opening angles, defined as the angle between two lines from the middle of the inner wall to the two tips of the inner wall, were measured from the photographs.

In addition, the initial lumen and outer diameters were measured from the images of the short ring segments cut from the ends of the arteries. Combined with the deformed outer diameters measured from the images taken under pressure, the deformed lumen diameters under pressure were determined using the incompressibility equations (18, 20).

2.7 *Histology*

Short arterial ring segments were cut pre- and post-collagenase treatment and fixed in 10% formalin overnight and processed for paraffin embedding. Thin sections ($\sim$5μm) were cut and processed for hematoxylin-eosin, and trichrome staining. The stained cross sections were examined under a microscope and photographed. From these images, the area of collagen was measured using Image-Pro Plus (version 4.5.1, 2002) and the collagen area to total tissue area ratio was determined from the photometric measurement to quantify the collagen content in the arterial wall.

2.8 *Statistical Analysis*

ANOVA test was used to determine the effects of collagenase treatment and the axial stretch ratio on the critical buckling pressure. A student t-test was used to
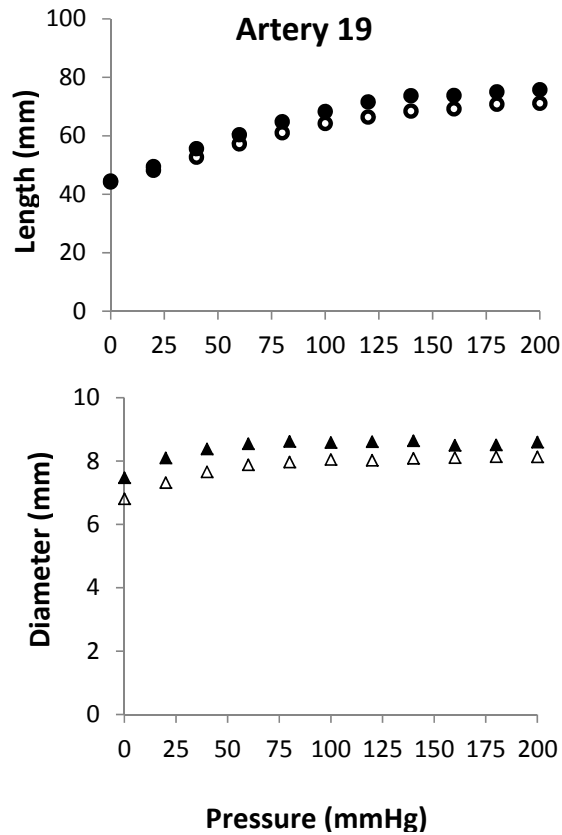
Figure 3: Deformations of an artery under lumen pressure. Axial length (circles, top panel) and outer diameter (triangles, bottom panel) plotted as functions of lumen pressure. Hollow and solid symbols represent data pre- and post- treatment (400U/ml), respectively.

compare the collagen contents and opening angles in arteries pre- and post- collagenase treatment. The significance level was set at a p value of 0.05.

3 Results

A total of thirteen porcine arteries were experimentally tested pre- and post- collagenase treatment at three concentrations (64U/ml, 128U/ml, and 400U/ml). The lengths, diameters, and wall thicknesses of all the arteries were measured before and after collagenase treatment and are summarized by group in Table 1. The mechanical properties, opening angle, and buckling pressure were determined pre-and

post- treatment and the results are described below.

Table 1: Summary of initial artery dimensions before and after collagenase treatment.

Group	Artery ID	Length (mm)	Outer Diameter (mm)	Wall Thickness (mm)
		Pre-treatment		
I (64U/ml)	10	63.7	5.70	0.671
	11	47.5	7.90	1.219
	12	28.5	9.92	0.882
II (320U/ml)	14	50.7	5.67	0.829
	15	41.2	5.71	0.719
	16	61.1	6.10	0.786
	17	60.0	6.22	0.727
III (400U/ml)	18	43.5	6.37	0.747
	19	45.5	6.81	0.817
	20	55.7	7.35	0.647
	21	56.2	4.94	0.525
	22	52.5	5.98	0.965
	23	73.2	6.92	0.751
mean ± SD, n = 13		**52.3 ± 11.4**	**6.6 ± 1.3**	**0.79 ± 0.17**
		Post-treatment		
I	10	62.9	6.02	0.671
	11	44.1	8.14	1.219
	12	28.2	9.47	0.882
II	14	49.5	5.67	0.829
	15	38.1	6.26	0.717
	16	57.5	6.24	0.786
	17	61.3	6.79	0.727
III	18	25.4	6.65	0.760
	19	43.8	7.48	0.975
	20	45.3	7.86	0.639
	21	52.7	5.28	0.780
	22	50.8	6.12	0.656
	23	72.4	7.80	0.976
mean ± SD, n =13		**48.6± 13.4**	**6.9± 1.2**	**0.82± 0.16**

3.1 Deformation under pressure and material constants

All arteries, pressurized while one end set free, expanded both longitudinally and circumferentially under increasing lumen pressure (see Fig. 3). The axial length was normalized with the initial length to convert to the axial stretch ratio and the outer diameter was averaged with lumen diameter and normalized with its initial value to convert to circumferential stretch ratios. The results showed that the axial stretch ratio increased consistently with increasing lumen pressure (Fig. 4). The mean axial stretch ratio was slightly higher post-treatment than pre-treatment. This trend was observed in all three groups, suggesting that the arteries weakened and deformed more after collagenase treatment. The circumferential stretch ratio first increased with lumen pressure, but then became nearly flat when the pressure exceeded ∼50 to 70 mmHg. The circumferential stretch ratio showed very little change post-collagenase treatment; suggesting that treatment had little effect on the stiffness in the circumferential direction.

The material constants of the Fung strain energy function were determined by fitting the pressure-outer diameter and pressure length curves with the pressure and axial tension equations (Eqs. 3 and 4). The results are summarized in Table 2 for all three groups before and after collagenase treatment.

3.2 The critical buckling pressure of arteries

Arteries were tested at different axial stretch ratio of λ_z = *1.1, 1.3, 1.5, and 1.7*, representing from sub-physiological (1.1 and 1.3), physiological (1.5 *in vivo*), to hyper-physiological (1.7) ranges. Buckling was seen in all arteries at all axial stretch ratios, except that four arteries did not buckle at stretch ratio of 1.7 within the tested pressure range of 300 mmHg (Table 3). The average critical buckling pressure decreased after collagenase treatment in all three groups (Fig. 5). The largest decrease was seen in Group III at an axial stretch ratio of 1.5, which was the normal stretch ratio in porcine carotid arteries in vivo (22).

The critical pressure at stretch ratios of 1.1, 1.3, and 1.5 before and after three collagenase treatments were analyzed using a two-way ANOVA test. The results showed that axial stretch ratio had a significant effect on the critical pressure in all groups (p<0.05). At the *in vivo* axial stretch ratio of 1.5, there was a significant difference between pre- and post-treatment in Group III. Groups II and III showed no significant difference between pre- and post-treatment.

The critical buckling pressure predicted by the buckling equation showed a fair estimate of our experimental critical buckling values before and after collagenase treatment for all groups (Fig. 6). The model correctly predicted that collagenase treatment would reduce the critical buckling pressure.

Table 2: Material property constants of all arteries before and after treatment.

Group	b_0	b_1	b_2	b_3	b_4	b_5	b_6
Pre-treatment							
	138.2	1.522	0.317	0.305	0.010	0.054	0.360
I (64U/ml)	221.7	0.352	0.019	0.001	0.172	0.001	0.170
	33.0	4.563	0.119	0.001	1.526	0.001	2.414
	1404.3	0.129	0.007	0.001	0.056	0.001	0.059
II (320U/ml)	981.8	0.170	0.006	0.001	0.086	0.001	0.089
	659.1	0.348	0.010	0.001	0.173	0.001	0.169
	584.7	0.610	0.043	0.080	0.257	0.001	0.145
	1127.7	0.217	0.006	0.016	0.276	0.001	0.229
	1063.3	0.518	0.001	0.001	0.283	0.001	0.339
	1126.8	0.664	0.001	0.001	0.409	0.001	0.480
III (400U/ml)	5116.7	0.145	0.002	0.010	0.083	0.001	0.073
	196.8	0.834	0.019	0.001	0.487	0.103	0.748
	4284.1	0.077	0.002	0.001	0.041	0.001	0.039
Post-treatment							
	512.0	0.432	0.011	0.001	0.171	0.001	0.264
I	1971.1	0.526	0.001	0.008	0.333	0.001	0.425
	5.6	8.503	0.074	0.001	4.207	0.001	4.942
	496.2	0.314	0.006	0.001	0.152	0.001	0.176
II	345.4	1.035	0.021	0.001	0.413	0.001	0.534
	11.8	3.945	0.060	0.001	2.420	0.324	2.931
	665.0	0.539	0.015	0.001	0.255	0.001	0.261
	1538.9	0.402	0.005	0.007	0.229	0.001	0.240
	3.2	0.001	0.001	7.885	3.398	0.001	0.030
	493.2	0.936	0.001	0.001	0.942	0.001	1.263
III	32.1	1.846	0.037	0.001	1.376	0.285	1.444
	38.8	6.562	0.044	0.001	3.189	0.008	4.036
	1148.7	0.177	0.001	0.001	0.111	0.001	0.090

3.3 Opening angle

The opening angles were obtained for arteries in group III before and after collagenase treatment. The average opening angle of the arteries ($n = 4$) was 36.5 ± 14.0 degrees pre-treatment and 50.0 ± 24.0 degrees post-treatment (Fig. 7). The collagenase treatment increased the opening angle though the difference was statistically insignificant.
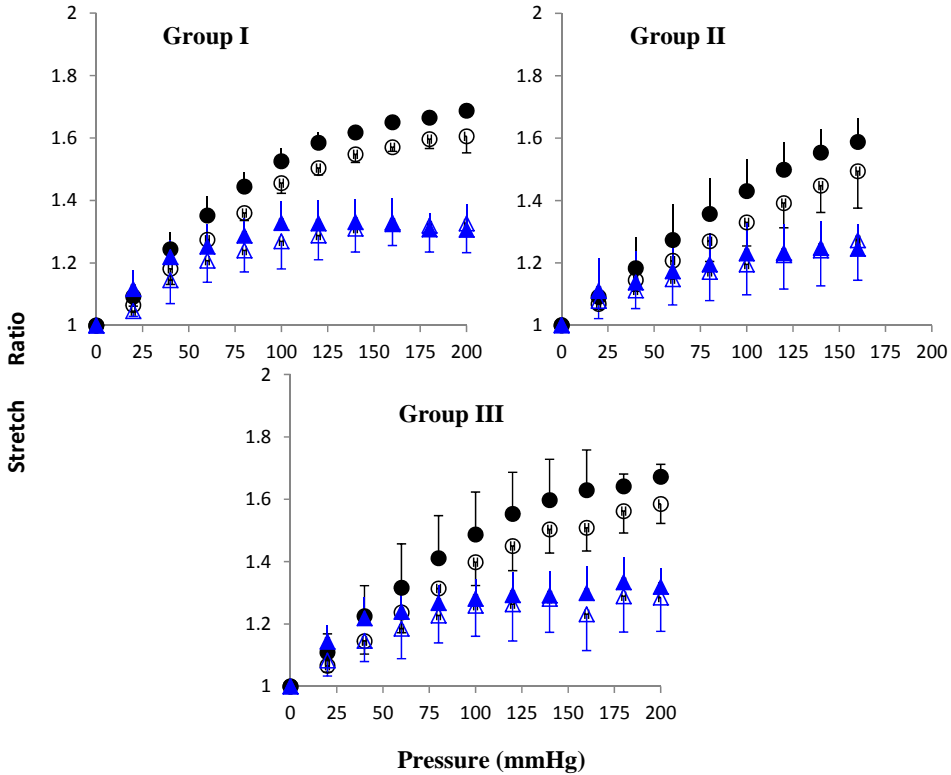
Figure 4: Axial (circles) and mid-wall circumferential (triangles) stretch ratios plotted as functions of lumen pressure. Hollow and solid symbols represent data pre- and post- treatment, respectively. Three panels shows data (*mean ± SD*) for arteries in group I (64*U/ml, n = 3*), group II (*128U/ml, n = 4*), and group III (*400U/ml, n = 6*).

3.4 The effects of collagenase on artery wall structure

Trichrome staining confirmed collagen degradation across the arterial wall after the collagenase treatment (Fig. 8). More distinct changes in collagen were seen in the arteries treated at the highest concentration (400 U/ml). Collagen content obtained by photometric measurement showed a significant decrease in group III post treatment ($p < 0.05$, Fig. 9).
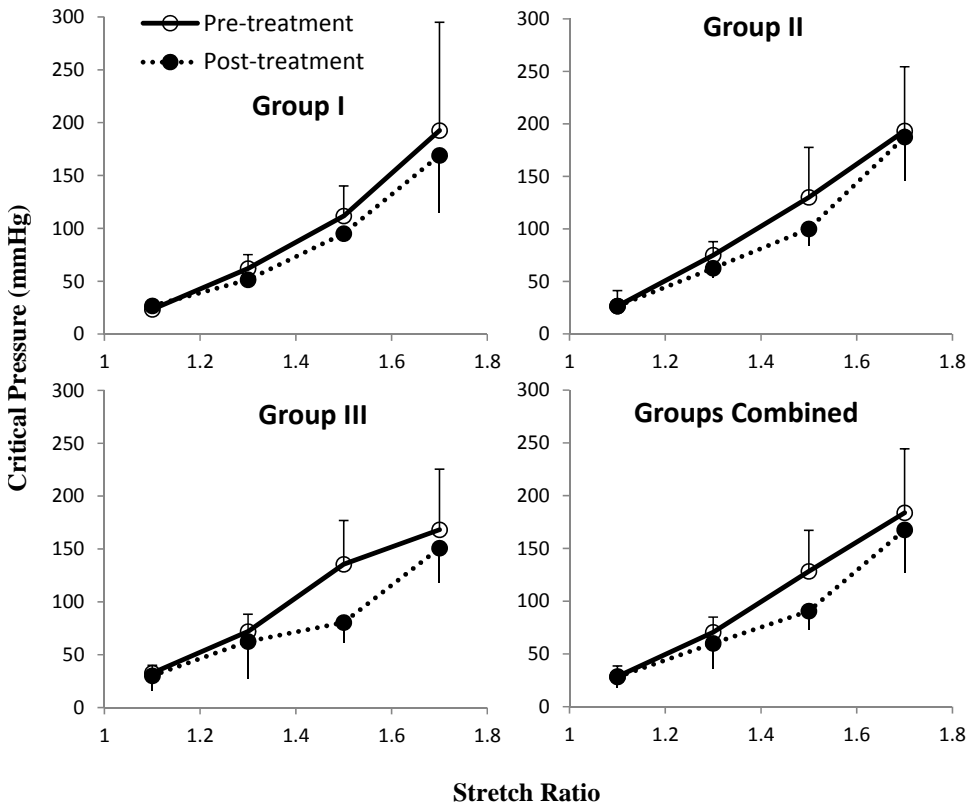
Figure 5: Experimental critical pressure (mean $\pm$ SD) for arteries of group I (64*U/ml, n = 3*), group II (*128U/ml, n = 4*), and group III (*400U/ml, n = 6*) pre- and post collagenase treatment. Bottom right consists of all groups together (*n = 13*). * p < 0.05 at stretch ratio 1.5 in Group III and Groups Combined.

4   Discussion

We studied the effects of collagenase treatment on the mechanical properties, the opening angle, and the critical buckling pressure of arteries. Our results showed that the critical buckling pressure and the stiffness of the porcine carotid arteries were reduced by collagenase treatments while the opening was increased after the treatment. The changes in collagen content and critical pressure were statistically significant in arteries treated at a high concentration (400U/ml) but not at lower concentrations. In addition, the buckling equation was found to yield a fair estimation to the experimentally measured critical pressures.
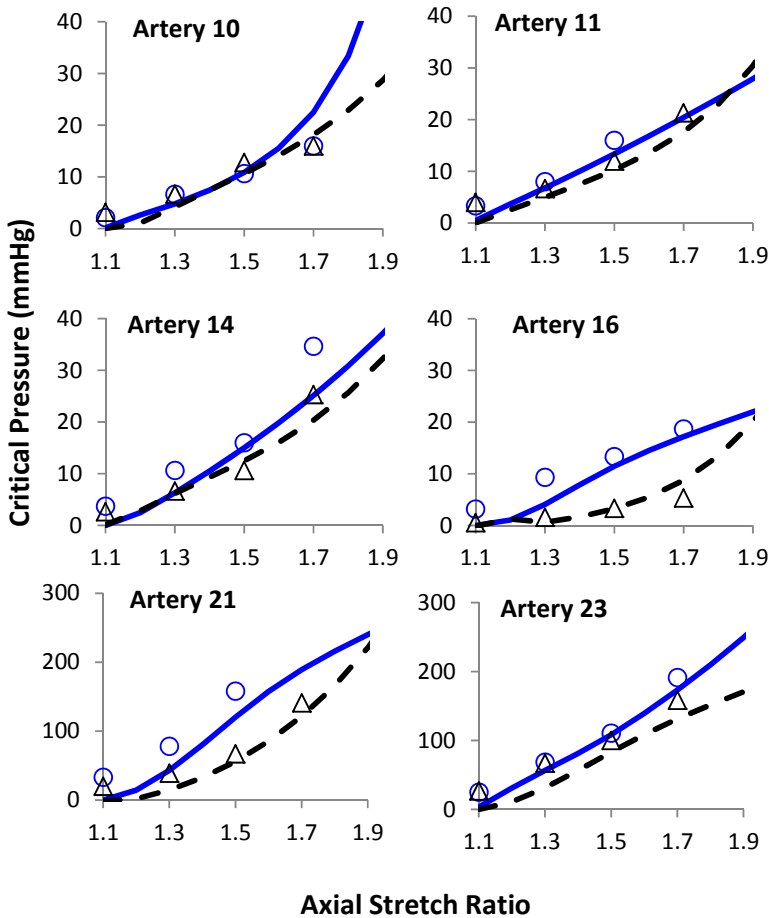
Figure 6: Model predicted critical pressures compared with experimental data for two representing arteries each in group I (*64U/ml, Top*), group II (*128U/ml, Middle*), and group III (*400U/ml,* bottom) The cycles and triangles represent data pre- and post- treatment, respectively. The solid and dotted lines represent the model predicted curves before and after collagenase treatments, respectively.

4.1   The effect of collagenase treatment on mechanical properties

In this study we showed that collagenase treatment caused an increase in the axial deformation but not in the circumferential deformation. This may be explained by the dominating circumferential alignment of collagen in the vessel wall (10). The orientation of elastic and collagen fibers, as well as smooth muscle cells together

Table 3: Experimental critical pressures before and after treatment.

Group	Artery ID	SR = 1.1,	1.3,	1.5,	1.7
		Pressures (mmHg)			
Pre-treatment					
	10	16	50	80	120
I (64U/ml)	11	25	60	120	NB*
	12	29	76	135	265
	14	28	80	120	260
	15	45	90	200	NB*
II (320U/ml)	16	24	70	100	140
	17	9	60	100	180
	18	39	95	198	NB*
	19	41	68	136	NB*
	20	23	45	76	103
III (400Uml)	21	33	78	158	NB*
	22	35	77	134	210
	23	25	69	111	191
Post-treatment					
	10	24	50	96	120
I	11	30	50	90	160
	12	26	54	99	227
	14	20	50	80	190
II	15	32	60	100	240
	16	24	70	100	140
	17	30	70	120	180
	18	57	130	NB*	NB*
	19	27	52	87	155
III	20	17	31	54	105
	21	20	39	67	141
	22	33	56	94	195
	23	27	67	100	158
NB*- No Buckling Observed					

constitute a continuous fibrous helix, which gives the media an ability to resist high loads in the circumferential direction. While collagenase treatment may equally breakdown the collagen fibers align in both the axial and circumferential directions, the ratio of change in the circumferential direction would be much smaller due to the large amount of collagen at baseline. While the overall weakening of the
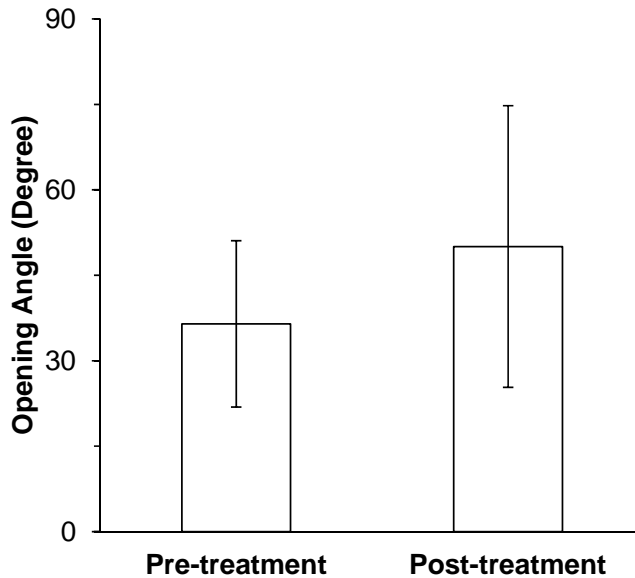
Figure 7: A comparison of opening angles of arteries (mean $\pm$ SD, n = 4) pre- and post-collagenase treatment (Group III, 400U/ml).

arterial wall observed is consistent with the results of Dobrin and colleagues, the spatial orientation is different. Dobrin and colleagues reported a reduction in wall stiffness in the circumferential direction of dog arteries post collagenase treatment (14). This difference may be due to the species difference, the concentration of collagenase used, or the difference in testing conditions (14, 23).

Studies done by Wagenseil et al (24) in elastin deficiency mouse arteries have shown that the arrangement and/or distribution of collagen and elastin fibers could lead to mechanical changes in the circumferential and longitudinal directions. Our histology results showed that arteries before treatment have organized collagen fibers arranged in a woven-helical pattern (media), but after collagenase treatment, the orientation of the collagen fibers become less wavy. These results indicate that collagenase treatment disrupts the organization of the collagen fibers, which is known to affect wall properties (24).

4.2   Effect of collagenase on critical buckling pressure

A new finding is that collagenase treatment tends to reduce the critical buckling pressure of porcine carotid arteries. Our previous model demonstrated that a decrease in wall stiffness reduces the critical pressure (18). An increase of axial
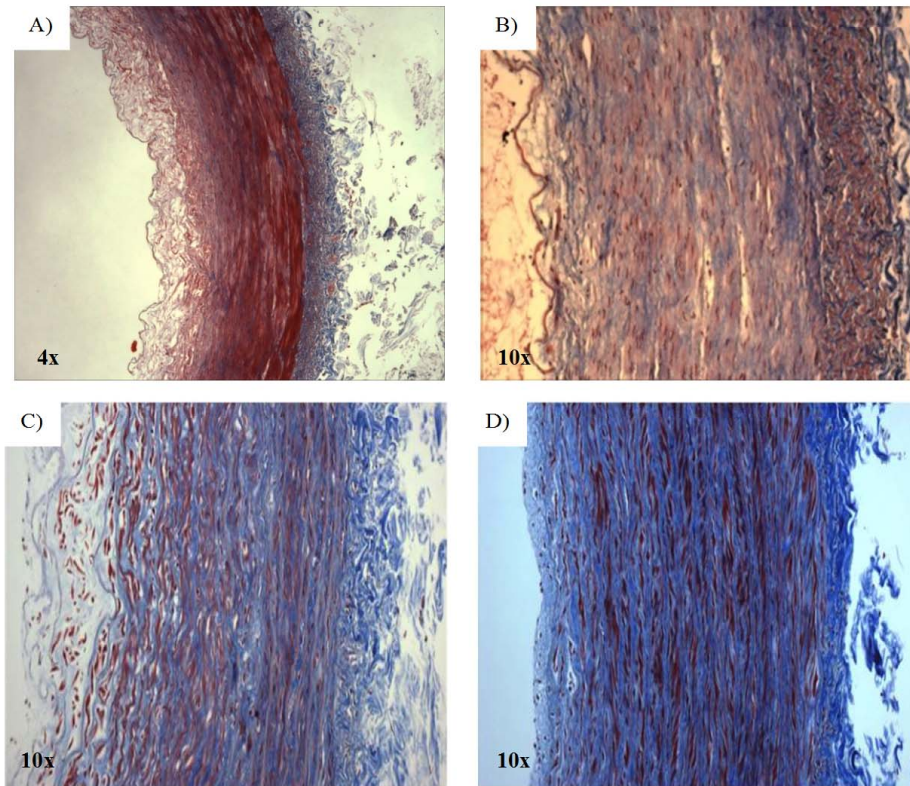
Figure 8: Micrographs (10x) of arterial cross sections with Trichrome collagen staining. A) artery 10 of Group I (64U/ml); B) artery 15 of group II (128U/ml); C) artery 18 of group III (128U/ml) and D) a normal artery (artery 18 before treatment).

deformation was observed in the collagenase treated arteries indicating a reduction of axial wall stiffness. This may be the reason for the observed reduction in critical pressure after collagenase treatment.

Previous studies in our lab demonstrated that elastin degradation due to elastase treatment significantly reduced the critical pressure of arteries (25). Compared to elastase treatment, collagenase treatment seems had less effect on the critical pressure. It is well known that collagen is not fully engaged in bearing wall stress at the low stress range. One possible explanation is that for long vessel segments, the wall stress at buckling is low so collagen is not fully engaged in the buckling deformation while elastin is engaged at the low stress level. In any regard, this and
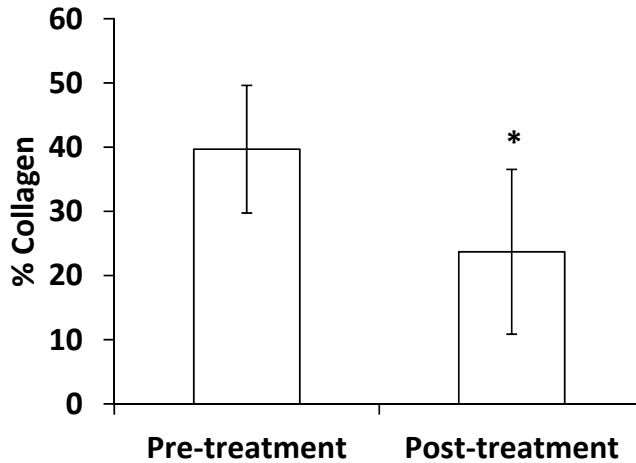
Figure 9: Comparison of collagen contents of arteries in group III (400U/ml) measured before and after collagenase treatment. A significant decrease in collagen content is seen (n=6, p < 0.05).

previous studies consistently demonstrated that degradation of extracellular matrix weakens the arterial wall, reduces wall stiffness, and thus leads to reduction in critical pressure, indicating arteries with weakened wall are prone to instability. The current results are also consistent with our previous results that arterial critical buckling pressure decreases with reduced axial strain (6, 9, 16).

4.3 Effect of collagenase on the opening angle

It has been well-known that when an arterial ring segment is cut, it springs open into c-shaped figurations due to the existence of residual stresses and strains within the wall (21, 26-29). Our current study demonstrated that collagenase treatment increased the arterial opening angle. An increase in the opening angle was also observed in porcine carotid arteries after elastase treatment in a previous study in our lab (25). These results are consistent with a previous report that rat saphenous arteries treated with elastase or collagenase increased the opening angle (30). However, another study showed that collagen degradation in bovine carotid arteries had little effect on the opening angle (31). These differences may be due to species difference.

4.4   Limitations

There were a few limitations in this study. First, all our experiments were performed under static loading conditions. Arteries *in vivo* are subjected to pulsatile pressure and the axial forces are due to the surrounding tissue tethering (32, 33). However, as our previous studies have shown that dynamic critical buckling pressure of arteries under pulsatile pressure is directly related to the static critical buckling pressure (34). The changes in static critical pressure due to collagenase treatment obtained in this study reflect the changes in critical pressure under pulsatile pressure *in vivo*. Second, the collagen degradation and collagen staining were nonspecific—the changes in different types of collagen in the wall were not differentiated. Third, our model did not account for vessel wall heterogeneity nor tissue support. The surrounding tissue support increases the critical pressure and make the artery buckling in higher order mode shapes (8). Additionally, our model analysis did not incorporate the opening angles. Our previous model simulations have demonstrated that opening angle had little effect on the critical pressure of arteries (16).

5   Conclusions

In conclusion, collagenase treatment weakens the arterial wall and reduces the critical buckling pressure of arteries. The current results extended our understanding of the collagenase effects from the previously known effects on wall mechanical stiffness and strength (14, 15) into the mechanical stability of arteries. This knowledge will be useful in understanding the physio-pathological change due to collagen degradation, deposition, and cross-linking in disease and ageing (11-13), especially those associated with artery tortuosity (3, 23).

References

1. Del Corso L, Moruzzo D, Conte B, Agelli M, Romanelli AM, Pastine F, Protti M, Pentimone F, & Baggiani G (1998) Tortuosity, kinking, and coiling of the carotid artery: expression of atherosclerosis or aging? *Angiology* 49(5):361-371.

2. Pancera P, Ribul M, Presciuttini B, & Lechi A (2000) Prevalence of carotid artery kinking in 590 consecutive subjects evaluated by Echocolordoppler. Is

there a correlation with arterial hypertension? *J Intern Med* 248(1):7-12.

3. Han HC (2012) Twisted Blood Vessels: Symptoms, Etiology, and Biomechanical Mechanisms. *J Vasc Res* 49(In press).

4. Aleksic M, Schutz G, Gerth S, & Mulch J (2004) Surgical approach to kinking and coiling of the internal carotid artery. *J Cardiovasc Surg (Torino)* 45(1):43-48.

5. Weibel J & Fields WS (1965) Tortuosity, Coiling, and Kinking of the Internal Carotid Artery. I. Etiology and Radiographic Anatomy. *Neurology* 15:7-18.

6. Han HC (2007) A biomechanical model of artery buckling. *J Biomech* 40(16):3672-3678.

7. Han HC (2009) The theoretical foundation for artery buckling under internal pressure. *J Biomech Eng* 131(12):124501.

8. Han HC (2009) Blood vessel buckling within soft surrounding tissue generates tortuosity. *J Biomech* 42(16):2797-2801.

9. Martinez R, Fierro CA, Shireman PK, & Han HC (2010) Mechanical buckling of veins under internal pressure. *Ann Biomed Eng* 38(4):1345-1353.

10. Holzapfel GA (2008) Collagen in arterial walls: biomechanical aspects. *Collagen: structure and mechanics*, ed Fratzl P (Spinger, New York).

11. Bode M (2000) Characterization of type I and type III collagens in human tissues. Dissertation (University of Oulu, Oulu).

12. Greenwald SE (2007) Ageing of the conduit arteries. *J Pathol* 211(2):157-172.

13. Kratky RG, Ivey J, & Roach MR (1999) Local changes in collagen content in rabbit aortic atherosclerotic lesions with time. *Atherosclerosis* 143(1):7-14.

14. Dobrin PB & Canfield TR (1984) Elastase, collagenase, and the biaxial elastic properties of dog carotid artery. *Am J Physiol* 247(1 Pt 2):H124-131.

15. Kitoh T, Kawai Y, & Ohhashi T (1993) Effects of collagenase, elastase, and hyaluronidase on mechanical properties of isolated dog jugular veins. *Am J Physiol* 265(1 Pt 2):H273-280.

16. Lee AY, Han B, Lamm SD, Fierro CA, & Han HC (2011) Effects of elastin degradation and surrounding matrix support on artery stability. *Am J Physiol Cell Physiol* (Expects online Dec. 9, 2011).

17. Martinez R (2011) Effect of collagenase treatment on arterial wall buckling. MS Master Thesis (University of Texas at San Antonio, San Antonio, TX).

18. Han HC (2008) Nonlinear buckling of blood vessels: a theoretical study. *J Biomech* 41(12):2708-2713.

19. Humphrey JD (2002) *Cardiovascular solid mechanics : cells, tissues, and organs* Springer, New York.

20. Fung YC (1990) *Biomechanics: Motion, Flow, Stress, and Growth* Springer, New York.

21. Han HC & Fung YC (1991) Species dependence of the zero-stress state of aorta: pig versus rat. *J Biomech Eng* 113(4):446-451.

22. Han HC, Ku DN, & Vito RP (2003) Arterial wall adaptation under elevated longitudinal stretch in organ culture. *Ann Biomed Eng* 31(4):403-411.

23. Dobrin PB, Schwarcz TH, & Baker WH (1988) Mechanisms of arterial and aneurysmal tortuosity. *Surgery* 104(3):568-571.

24. Wagenseil JE, Nerurkar NL, Knutsen RH, Okamoto RJ, Li DY, & Mecham RP (2005) Effects of elastin haploinsufficiency on the mechanical behavior of mouse arteries. *Am J Physiol Heart Circ Physiol* 289(3):H1209-1217.

25. Lee AY (2011) Determing The Critical Buckling Pressure of Blood Vessels Through Modeling and In Vitro Experiments Doctor of Philosophy in Biomedical Engineering Dissertation (The University of Texas at San Antonio, San Antonio, TX).

26. Liu SQ & Fung YC (1988) Zero-stress states of arteries. *J Biomech Eng* 110(1):82-84.

27. Vaishnav RN & Vossoughi J (1987) Residual stress and strain in aortic segments. *J Biomech* 20(3):235-239.

28. Fung YC (1984) *Biodynamics: Circulation* Springer-Verlag; 1st Ed.

29. Han HC, Marita S, & Ku DN (2006) Changes of opening angle in hypertensive and hypotensive arteries in 3-day organ culture. *J Biomech* 39(13):2410-2418.

30. Zeller PJ & Skalak TC (1998) Contribution of individual structural components in determining the zero-stress state in small arteries. *J Vasc Res* 35(1):8-17.

31. Greenwald SE, Moore JE, Jr., Rachev A, Kane TP, & Meister JJ (1997) Experimental investigation of the distribution of residual strains in the artery wall. *J Biomech Eng* 119(4):438-444.

32. Learoyd BM & Taylor MG (1966) Alterations with age in the viscoelastic properties of human arterial walls. *Circ Res* 18(3):278-292.

33. Han HC & Fung YC (1995) Longitudinal strain of canine and porcine aortas. *J Biomech* 28(5):637-641.

34. Liu Q & Han HC (2011) Mechanical buckling of artery under pulsatile flow. *ASME Summer Bioengineering Conference*. Farmington, PA. June 2011.